DAMAGE DETECTION OF A ROTATING CRACKED SHAFT USING AN ACTIVE MAGNETIC BEARING AS A FORCE ACTUATOR

Girindra Mani D. Dane Quinn*
Department of Mechanical Engineering
The University of Akron
Akron, OH 44325–3903

Travis Bash Mary E. F. Kasarda
Daniel J. Inman R. Gordon Kirk
Department of Mechanical Engineering
Virginia Tech
Blacksburg, VA 24061–0238

ABSTRACT

We consider the active health monitoring of rotordynamic systems in the presence of breathing shaft cracks. The shaft is assumed to be supported by conventional bearings and the Active Magnetic Bearing (AMB) is used in a mid-shaft or outboard location as an actuator to apply specified, time-dependent forcing on the system. These forces, if properly chosen, induce a combination resonance that can be used to identify the magnitude of the time-dependent stiffness arising from the breathing mode of the shaft crack.

1 INTRODUCTION

Many critical rotating machines such as compressors, pumps, and gas turbines continue to be used despite aging and the associated potential for damage accumulation. Therefore, the ability to monitor the structural health of these systems is becoming increasingly important. In the most general terms, *structural health monitoring* can be defined as the process of implementing a damage-detection strategy. This process involves the observation of a structure over a period of time, the extraction of features from these measurements, and the analysis of these features to determine the current state of health of the system. In this study, we present a novel health monitoring approach for the detection of cracks in rotating shafts utilizing an Active Magnetic Bearing (AMB) as an actuator for applying multiple types of force inputs on to a rotating structure for analysis of associated outputs. The AMB is used in conjunction with conventional support bearings and is not utilized for rotor support, although it is expected that the technique can be applied to rotors under full magnetic levitation. In addition to early crack detection, the technique described here lays the foundation for self-healing of some cracks using the AMB actuator to apply forces at intervals to prevent a crack from "breathing."

In last two decades, there have been a growing number of applications for AMBs. However, in the majority of these the AMBs are used as active suspension systems for shafts or rotors. Several components of an AMB are characterized by non-linear behavior and therefore the entire system is inherently nonlinear [2]. Zhu et al. [1] examine how the AMB, used as a damper, can also actively control the vibration of rotor systems and improve their stability. Much of the previous research work is focused on the suspension characteristics and the stability of the AMBs. In contrast, this work uses AMBs strictly an excitation device.

Much work has also been done over the years regarding crack mechanics and damage detection. Dimarogonas [3] gives an excellent review on the vibration of cracked structures. However, a consistent cracked bar vibration theory is yet to be developed, particularly with regards to breathing cracks. Wauer [4] discusses many investigations into the dynamics of cracked rotors where the author mentions the lack of theories on crack detection in its initial stage. Plaut [5] analyzed four resonances arising from internal, flexural and torsional frequencies. However, they only considered vibrations of unbalanced rotating shaft with no crack in it. Qin et al. [6] discuss the dynamic response of a cracked shaft taking swing vibration of a disc into consideration. They characterize how the response becomes chaotic due to

*quinn@uakron.edu

new resonances as the crack deepens.

The current work is focused on the investigation on the vibrational response of a cracked rotating shaft. A phenomenological model has been developed that incorporates the breathing of the crack, nonlinear shaft bending stiffness, and the external forces from the AMBs. This model is then analyzed and a combination resonance is identified and the dynamical behavior when the system is operated at this resonance can be used to quantify the damage of the shaft.

2 MODEL

2.1 Equations of motion

The equations of motion for a simple rotor with a cracked shaft can be written as [3, 7]:

$$\mathbf{M}\,\ddot{\mathbf{u}} + \mathbf{C}\,\dot{\mathbf{u}} + \mathbf{K}(\mathbf{u},t)\,\mathbf{u} = \mathbf{F}_{\mathrm{g}} + \mathbf{F}_{\mathrm{AMB}}, \qquad (1)$$

where:

$$\mathbf{M} = \begin{pmatrix} m & 0 \\ 0 & m \end{pmatrix}, \quad \mathbf{C} = \begin{pmatrix} c & 0 \\ 0 & c \end{pmatrix},$$

$$\mathbf{K} = \begin{pmatrix} k_{11} & k_{12} \\ k_{21} & k_{22} \end{pmatrix}, \quad \mathbf{u} = \begin{pmatrix} u_z \\ u_y \end{pmatrix}, \quad \mathbf{F}_{\mathrm{g}} = \begin{pmatrix} mg \\ 0 \end{pmatrix}.$$

$\mathbf{F}_{\mathrm{g}}$ represents the gravitational force and $\mathbf{F}_{\mathrm{AMB}}$ is the external force vector from the AMB. Finally, the shaft is assumed to be rotating at constant angular speed $\hat{\Omega}$.

The stiffness matrix can be written as:

$$\mathbf{K}(\mathbf{u},t) = \mathbf{K}_0(\mathbf{u},t) + \mathbf{\Delta K}(\mathbf{u},t), \qquad (2)$$

where $\mathbf{K}_0$ represents the stiffness matrix of uncracked shaft and $\mathbf{\Delta K}$ is the additive stiffness matrix that describes the change in shaft stiffness with increasing damage. Typically the stiffness of the shaft is reduced with increasing damage and this degradation grows with increasing damage. Although we seek to relate the dynamics of this model to the magnitude of the shaft crack we make no attempt here to relate the crack geometry with changes in stiffness. Instead we focus on the dynamical behavior of the system as the stiffness changes.

The displacement vector can also be decomposed as:

$$\mathbf{u}(t) = \mathbf{u}_0 + \mathbf{u}_1(t), \qquad (3)$$

where $\mathbf{u}_0$ is the static deflection of the uncracked shaft due to gravity.In terms of $\mathbf{u}_1$ the equations of motion become:

$$\mathbf{M}\,\ddot{\mathbf{u}}_1 + \mathbf{C}\,\dot{\mathbf{u}}_1 + (\mathbf{K}_0 + \mathbf{\Delta K})\,\mathbf{u}_1 = -\mathbf{\Delta K}\,\mathbf{u}_1 + \mathbf{F}_{\mathrm{AMB}}. \qquad (4)$$

The small vibrational movement will not affect the additive stiffness matrix provided $|\mathbf{u}_0| \gg |\mathbf{u}_1(t)|$. Therefore, $\mathbf{\Delta K}$ can be assumed to be periodically time-variant.

2.2 Shaft Stiffness

For a breathing crack, which opens and closes once per shaft revolution, the stiffness matrix is periodically time-varying. Unfortunately, the development of an exact stiffness model of a "breathing" crack from a fundamental model is quite complicated. Instead, the stiffnesses in rotating coordinate system (ξ, η) are considered to be [7]:

$$\begin{pmatrix} k_\xi \\ k_\eta \end{pmatrix} = \begin{pmatrix} k_0 - \Delta k_\xi \,\frac{1+\cos(\theta)}{2} \\ k_0 - \Delta k_\eta \,\frac{1+\cos(\theta)}{2} \end{pmatrix}. \qquad (5)$$

ξ is the crack direction coordinate and η is the cross-crack direction coordinate. θ is the angle between Δu and ξ directions. Δk_ξ and Δk_η are the reduction of stiffness at fully open crack in ξ and η directions respectively. These quantities can be either experimentally determined or empirically related to the crack length and hence the "health" of the shaft. For small cracks (less than the radius of the shaft), k_η can be approximated as simply k_0 [7] and the stiffness matrix of the cracked rotor in the stationary coordinate system can be written as:

$$\mathbf{K} = k_0 \begin{pmatrix} 1 & 0 \\ 0 & 1 \end{pmatrix} - \frac{\Delta k_\xi}{4} \begin{pmatrix} f(\theta) & g(\theta) \\ g(\theta) & h(\theta) \end{pmatrix},$$

where:

$$\begin{aligned} f(\theta) &= 1 + \frac{3}{2}\cos(\theta) + \cos(2\,\theta) + \frac{1}{2}\cos(3\,\theta), \\ &= \sum_{n=0}^{N} p_n\ \cos(n\theta), \\ g(\theta) &= \frac{1}{2}\sin(\theta) + \sin(2\,\theta) + \frac{1}{2}\sin(3\,\theta), \\ &= \sum_{n=0}^{N} q_n\ \sin(n\theta), \\ h(\theta) &= 1 + \frac{1}{2}\cos(\theta) - \cos(2\,\theta) - \frac{1}{2}\cos(3\,\theta), \\ &= \sum_{n=0}^{N} r_n\ \cos(n\theta). \end{aligned}$$

2.3 Harmonic AMB Forcing

The critical frequency of the shaft oscillations is $\sqrt{k_0/m}$. The opening and closing of the crack, synchronous with the rotational speed $\hat{\Omega}$ of the shaft, introduces a time-varying stiffness. Further, assume that the AMB forcing varies harmonically, so that:

$$\mathbf{F}_{\mathrm{AMB}} = \begin{pmatrix} F_{0,z}\cos(\hat{\Omega}_2\ t) \\ 0 \end{pmatrix}.$$

Notice that forcing is applied in the z direction only. Scaling the coordinates by the static displacement $\delta_{st} = mg/k_0$ and time with the critical frequency, so that $\tau = \sqrt{k_0/m}\ t$, the equations of motion become:

$$\begin{pmatrix} \ddot{z} \\ \ddot{y} \end{pmatrix} + \epsilon\ \kappa \begin{pmatrix} \dot{z} \\ \dot{y} \end{pmatrix} + \begin{pmatrix} z \\ y \end{pmatrix} + \epsilon \begin{pmatrix} \alpha_1 z^3 \\ \alpha_2 y^3 \end{pmatrix} - \epsilon\ \beta \begin{pmatrix} f(\Omega\ \tau) & g(\Omega\ \tau) \\ g(\Omega\ \tau) & h(\Omega\ \tau) \end{pmatrix} \begin{pmatrix} z \\ y \end{pmatrix} = \epsilon\beta \begin{pmatrix} f(\Omega\ \tau) \\ g(\Omega\ \tau) \end{pmatrix} + \begin{pmatrix} \gamma \cos(\Omega_2\ t) \\ 0 \end{pmatrix}. \quad (6)$$

with:

$$\Omega = \frac{\hat{\Omega}}{\sqrt{k_0/m}}, \quad \Omega_2 = \frac{\hat{\Omega}_2}{\sqrt{k_0/m}},$$
$$\epsilon\beta = \frac{\Delta k_\xi}{4\ k_0}, \quad \epsilon\zeta = \frac{c}{\sqrt{k_0\ m}}, \quad \gamma = \frac{F_{0,z}}{k_0\ \delta_{st}}.$$

The magnitude of the time-varying stiffness is $\epsilon\ \beta$. Moreover, β is identified as the "damage" parameter because it represents the magnitude of the stiffness degradation assumed to scale with the damage in the shaft. Finally, the AMB forces appear in the model as external excitation, of amplitude γ and frequency Ω_2. The quantity ϵ is simply a nondimensional scaling parameter used to indicate the relative sizes of the various parameters.

The resulting mathematical model can be described as a two coupled nonlinear equations with both parametric and external excitation. In the analysis that follows, a combination resonance is identified between the critical shaft frequency, the shaft rotational speed, and the external frequency of the AMB excitation. The amplitude of the oscillations at this resonant operation is proportional to both the magnitude of the external excitation γ and, more importantly, the magnitude of the shaft damage, described by the nondimensional quantity $\epsilon\beta$ in the above equation. Finally, this response is sensitive to changes in Ω_2, the frequency of the AMB excitation. This is expected to provide a means of identifying marginal damage states.

3 MULTIPLE SCALE ANALYSIS

Multiple scale analysis [8] is applied to analyze the dynamical behavior of Eqs. (6). Assuming the solution to these equations takes the form $\mathbf{u}_1 = u_{1,0} + \epsilon\ u_{1,1} + \cdots$, then the first order solution takes the form:

$$z_0 = A_1(\eta)\cos\left(\tau + \phi_1(\eta)\right) + \Gamma\ \cos(\Omega_2\ \tau), \quad (7)$$
$$y_0 = A_2(\eta)\cos\left(\tau + \phi_2(\eta)\right) \quad (8)$$

where:

$$\eta = \epsilon\ \tau, \quad \Gamma = \frac{\gamma}{1 - \Omega_2^2}.$$

	Resonance Condition	Description
1	$\Omega = \frac{1}{3}, \frac{1}{2}, \frac{2}{3}, 1, 2$	parametric
2	$\Omega_2 = 1, 3$	external
3	$\Omega_2 = \lvert n\Omega - 1\rvert$ $n = 1, 2, 3$	combination

Table 1: Resonant forcing conditions.

Note that η represents a slow time-scale. The slowly varying amplitude and phase, A_i and ϕ_i respectively, are determined from the slow flow equations obtained from the $\mathcal{O}(\epsilon^1)$ equations by equating the secular terms to zero. However, in this system secular terms only appear for resonant forcing conditions, as shown in Table 1. This work focuses on the combination resonance as a mechanism for identifying the damage parameter. Specifically, can we estimate the magnitude of the damage parameter β by varying only Ω_2 and γ—the parameters associated with the external AMB forcing?

The first resonance condition depends on Ω and β. However, we assume no control over Ω so that this condition cannot be imposed. Therefore the AMB forcing cannot be varied to satisfy the first condition (parametric resonance). Second resonance condition does depends on Ω_2. However, the predicted response from the multiple scales analysis is independent of the damage parameter, β. This condition cannot be used to characterize the magnitude of β from vibration data.

For $\Omega_2 = \Omega_2^\star \equiv |n\ \Omega - 1|$, the combination resonance condition can be satisfied for any value of Ω, the rotational speed of the shaft. Moreover, the amplitude of the response scales linearly with β. Upon application of the method of multiple scales, the resulting slow flow equations in the z direction can be written as:

$$\frac{dA_1}{d\eta} = -\frac{1}{\Omega_2^\star}\left[\Gamma_{z,n}\ \sin\phi_1 + \frac{\zeta\ A_1}{2}\right],$$
$$\frac{d\phi_1}{d\eta} = -\frac{1}{\Omega_2^\star}\left[\frac{\Gamma_{z,n}}{A_1}\ \cos\phi_1 - \frac{\sigma_2}{\Omega_2^\star} - \frac{3\ \alpha_1}{4}\ \left(\frac{A_1^2}{2} + \Gamma^2\right) + \frac{\beta\ p_0}{2}\right],$$

where σ_2 is the detuning from the exact resonance, that is $\Omega_2 = \Omega_2^\star + \epsilon\ \sigma_2$, and:

$$\Gamma_{z,n} = \frac{p_n}{4}\ \Gamma\ \beta.$$

Similar results can be derived for the vibration amplitude in the y direction.

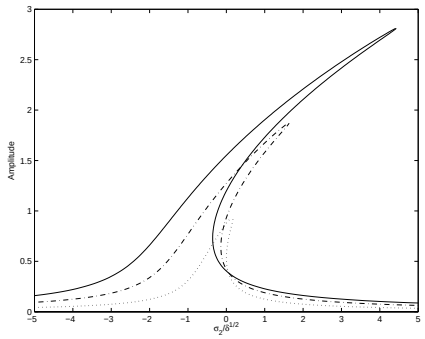

Figure 1: Damage effect on response amplitude versus detuning curves $\beta = 1.5$ (solid), 1.0 (dash-dotted), 0.5 (dotted) ($\alpha_1 = 1.0$, $\gamma = 1.5$, $\zeta = 0.2$, $\Omega = 2\pi$, $\Omega_2 = 2$).

Stationary solutions of the original Eqs. (6) correspond to equilibrium points in this system. From this, the amplitude-detuning relationship is obtained as:

$$\frac{\sigma_2}{\Omega_2^\star} = \frac{\beta\ p_0}{2} - \frac{3\ \alpha_1}{4}\left(\frac{{A_1}^2}{2} + \Gamma^2\right) \pm \sqrt{\frac{\Gamma_{z,n}^2}{A_1^2} - \frac{\zeta^2}{4}}, \quad (9)$$

and one may also solve for the stationary phase ϕ_1. In the absence of the nonlinearity ($\alpha_1 = 0$), the response amplitude becomes:

$$A_1 = \sqrt{\frac{p_n\ \Gamma\ \beta}{\zeta^2 + \left(2\frac{\sigma_2}{\Omega_2^\star} - \beta\ p_0\right)^2}}.$$

Unfortunately, for $\alpha_1 \neq 0$ the relationship between A_1 and σ_2 cannot be inverted to determine A_1 in terms of σ_2. Instead, Eq. (9) is solved numerically for A_1 and representative results are shown in Figure 1.

The maximum amplitude of the response is determined to be:

$$A_1^\star = \frac{2\ \Gamma_{z,n}}{\zeta} = \left(\frac{p_n\ \Gamma}{2\ \zeta}\right)\beta, \quad (10)$$

which occurs at a detuning:

$$\frac{\sigma_2^\star}{\Omega_2^\star} = \frac{\beta\ p_0}{2} - \frac{3\ \alpha_1\ \Gamma^2}{8}\left(\left(\frac{p_n\ \beta}{2\ \zeta}\right)^2 + 2\right). \quad (11)$$

Thus the when the combination resonance is excited the amplitude of the observed vibrations that occur at the critical frequency of the shaft scale with β, the damage parameter. The maximum amplitude can be used to detect and quantify the damage. Notice that the maximum amplitude of the response scales linearly with β and is independent of α_1, the strength of the nonlinearity.

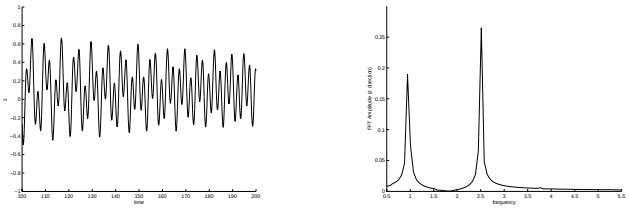

Figure 2: z direction response and its FFT ($\alpha = 1.0$, $\beta = 1.0$, $\gamma = 1.5$, $\zeta = 0.2$, $\Omega = 2\pi$, $\Omega_2 = 2.5$).

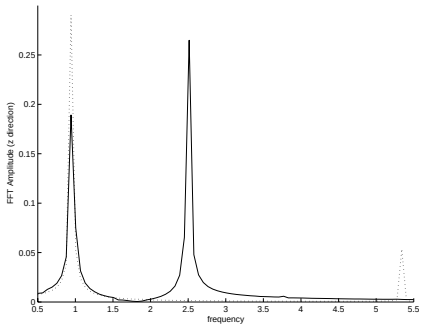

Figure 3: Comparison of the FFT amplitudes at resonant and non-resonant forcing frequencies with $\Omega_2 = 2.5$ (solid) and $\Omega_2 = 5.338$ (dashed) ($\alpha = 1.0$, $\beta = 1.0$, $\gamma = 1.5$, $\zeta = 0.2$, $\Omega = 2\pi$).

4 FOURIER ANALYSIS

Numerical solutions of Eqs. (6) are obtained using a 4^{th}-order Runge-Kutta algorithm. Figure (2) depicts an instance of such solution in the z directions. Also, a Fast Fourier Transform (FFT) is used to quantify the amplitude variation with respect to the variation of different system parameters. Notice that the FFT of the solution in the z direction has two peaks: one at shaft critical frequency and a second at the external excitation frequency.

4.1 Excitation at combination resonance

We present a novel approach to quantify the shaft damage by relating the amplitude of the vibration response with the damage parameter β. In Eqs. (6), we make use of the combination resonance condition as shown in Figure (3)—the amplitude at the resonant external frequency ($\Omega_2 \cong 5.3$) is considerably higher than that at an arbitrary frequency ($\Omega_2 = 2.5$) away from the resonant frequency. It is noted that (i) rotational speed Ω is assumed to be away from the parametric resonant frequency, and (ii) Ω_2 is chosen such that it is away from external resonant frequency (see Table 1) to avoid additional resonant interactions.

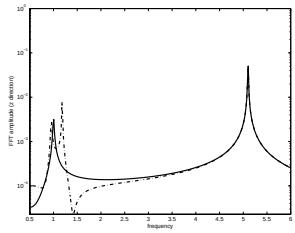

a. $\Omega_2 = 5.1$

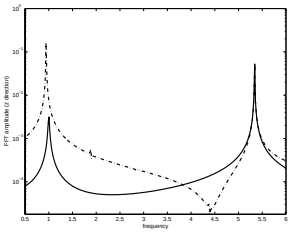

b. $\Omega_2 = 5.34$

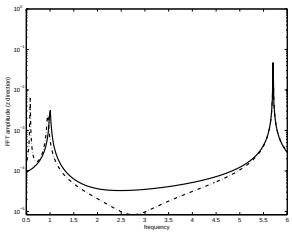

c. $\Omega_2 = 5.7$

Figure 4: Comparison of FFT amplitudes below, at and above resonant forcing frequencies for both undamaged and damaged systems ($\alpha = 1.0$, $\gamma = 1.5$, $\zeta = 0.2$, $\Omega = 2\pi$). Solid and dashed lines represent undamaged ($\beta = 0$) and damaged ($\beta = 1.0$) systems respectively.

4.2 Proposed resonance based approach

In both healthy and damaged systems a peak will occur at the critical frequency. However, we are interested in the variation of the magnitude at the frequency as system moves from undamaged to to damaged state. This is demonstrated in Figure 4. Three excitation frequencies were chosen at and around the combination resonance: $\Omega_2 = 5.1$ (below resonance), $\Omega_2 = 5.34$ (resonance), and $\Omega_2 = 5.7$ (above resonance). Expectedly, both undamaged and damaged systems show a peak at critical frequency. The difference in the magnitude, however, is very significant. The magnitude at the excitation frequency is same for both undamaged and damaged cases. We also observe that FFT magnitude at forcing frequency is insensitive to either change in the forcing frequency, or damage status of the system.

In Figure 4 there can also be seen a slight shift in the critical frequency with increasing damage as a direct result of variation of the shaft stiffness. The crack leads to a reduction in stiffness and an increase in damping [9], which in turn leads to changes in natural frequencies (as happens to the critical frequency here), modal damping and modal shape components. While this aspect of the response (variation in modal quantities) has been used as a tool to identify and quantify damage [10, 11, 12], the dynamical behavior induced by the combination resonance is much more sensitive to the damage parameter β.

Therefore, usage of combination resonance condition shows very promising results. To strengthen our premise, the damage sensitivity of the time-series needs to be determined at other frequencies. Each of the three lines in the Figure 5 shows the maximum of the difference between the damaged and the undamaged magnitudes in the in the vicinity of resonant forcing frequency ($\Omega_2 = 5.34$). The figure clearly shows that when the system is not excited at resonant frequency, damage sensitivity is nearly negligible—the maximum damaged and undamaged FFT amplitudes are nearly identical. Only near the resonant forcing is the response sensitive to the damage.

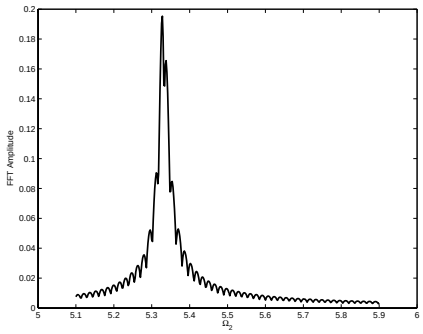

Figure 5: Maximum of difference between damaged FFT amplitude and undamaged FFT amplitude in the vicinity of resonant forcing frequency ($\alpha = 1.0$, $\beta = 0.0, 1.0$, $\gamma = 1.5$, $\zeta = 0.2$, $\Omega = 2\pi$).

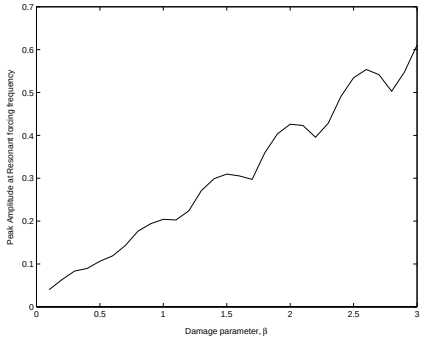

Figure 6: Peak at resonance as damage grows ($\alpha = 0.5$, $\gamma = 1.5$, $\zeta = 0.2$, $\Omega = 2\pi$).

Because of the nature of the dynamic system, this peak value (vibration amplitude) is sensitive to the damage of the shaft, quantitatively, the size of the crack (β). Intuitively, one expects higher (in amplitude) vibration for higher value of β. If the peak amplitude values are plotted against the damage parameter β, a nearly linear relationship is seen in Figure 6. This is in agreement with the prediction by the multiple scale analysis.

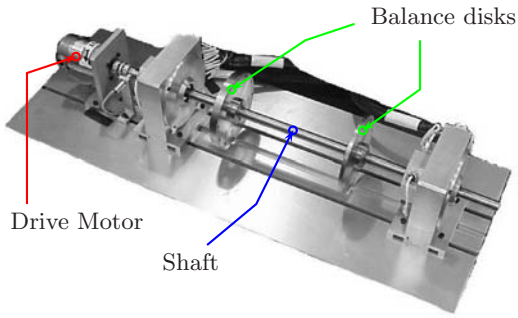

Figure 7: Active magnetic bearing test rig used for shaft crack testing.

5 EXPERIMENTAL TEST RIG

A test rig is currently under development to experimentally investigate new crack shaft detection procedures described here. The test rig uses a steel shaft with two balance disks, and is supported in rolling element bearings at the inboard and outboard locations. The test assembly shaft has a constant diameter of 15.9 mm (0.625 in) and a bearing span of 558.8 mm (22 in). One or two AMB actuators can be retrofit at almost any axial location for their use in the new health monitoring approach. Each AMB is an 8-pole radial heteropolar design with an air gap of 0.38 mm (0.015 in) and a load capacity of 66.5 N (30 lbs). In addition, the magnetic stator is 60.3 mm (2.375 in) long, and has an inner diameter of 47.6 mm (1.875 in). The partial test rig assembly is shown in Figure 7. Multiple rotor shafts with various crack configurations will be placed in the test rig for investigation of the new health monitoring techniques. Initially, shafts with notches representing cracks will be examined, followed by an attempt to create a breathing crack scenario by using a wire Electrical Discharge Machine (EDM).

The new health monitoring procedure involves examining rotor responses (outputs) due to multiple inputs from the AMB actuators. This is similar to traditional modal analysis techniques except that now the structure under investigation is rotating, and the input from the actuator can be a traditional "impact" or more complex such as a sinusoidal force input of varying frequency and/or amplitude. The ability of the actuator to provide multiple repeatable force inputs to the system allow for significantly more useful monitored data for applying advanced analysis techniques like the approach described here.

ACKNOWLEDGEMENT

This material is based upon work supported by the National Science Foundation under Grant No. CMS–0219701.

REFERENCES

[1] Zhu, C., Robb, D. A., and Ewins, D. J., 2003, "The Dynamics of a Cracked Rotor with an Active Magnetic Bearing," J. Sound Vib., **265** (3), pp. 469–487.

[2] Ji, J. C., and Hansen, C. H., 2001, "Nonlinear Oscillations of a Rotor in Active Magnetic Bearings," J. Sound Vib., **240** (4), pp. 599–612.

[3] Dimarogonas, A. D., 1996, "Vibration of Cracked Structures: A State of the Art Review," Engineering Fracture Mechanics, **55** (5), pp. 831–857.

[4] Wauer, J., 1990, "Dynamics of Cracked Rotors: A Literature Review," Appl. Mech. Reviews, **43** (1), pp. 13–18.

[5] Plaut, R. H., and Wauer, J., 1995, "Parametric, External, and Combination Resonances in Coupled Flexural and Torsional Oscillations of an Unbalanced Rotating Shaft," J. Sound Vib., **183** (5), pp. 889–897.

[6] Qin, W. Y., Meng, G., and Zhang, T., 2003, "The Swing Vibration, Transverse Oscillation of Cracked Rotor and The Intermittence Chaos," J. Sound Vib., **259** (3), p. 2003.

[7] Gasch, R., 1993, "A Survey of the Dynamic Behavior of a Simple Rotating Shaft with a Transverse Crack," J. Sound Vib., **160** (2), pp. 313–332.

[8] Nayfeh, A. H., and Mook, D. T., 1979, *Nonlinear Oscillations*, John Wiley & Sons, Inc., New York.

[9] Adams, R. D., Walton, D., Flitcroft, J. E., and Short, D., 1975, "Vibration testing as a nondestructive test tool for composite materials," Composite Reliability, ASTM STP, **580**, pp. 159–175.

[10] Capecchi, D., and Vestroni, F., 1999, "Monitoring of Structural Systems by Using Frequency Data," Earthquake Engng. Struct. Dyn., **28**, pp. 447–461.

[11] Nandwana, B. P., and Maiti, S. K., 1997, "Detection of the Location and Size of a Crack in Stepped Cantilever Beams Based on Measurements of Natural Frequencies," J. Sound Vib., **203** (3), pp. 435–446.

[12] Lee, Y.-S., and Chung, M.-J., 2000, "A study on crack detection using eigenfrequency test data," Computer and structures, **77**, pp. 327–342.